

## Probing unconventional superconducting symmetries using Josephson interferometry

W. K. Neils, D. J. Van Harlingen, S. Oh, J. N. Eckstein, German Hammerl, Jochen Mannhart, Andreas Schmehl, Christof W. Schneider, Robert R. Schulz

### Angaben zur Veröffentlichung / Publication details:

Neils, W. K., D. J. Van Harlingen, S. Oh, J. N. Eckstein, German Hammerl, Jochen Mannhart, Andreas Schmehl, Christof W. Schneider, and Robert R. Schulz. 2002. "Probing unconventional superconducting symmetries using Josephson interferometry." *Physica C: Superconductivity* 368 (1-4): 261-66.  
[https://doi.org/10.1016/S0921-4534\(01\)01178-9](https://doi.org/10.1016/S0921-4534(01)01178-9).

## Probing unconventional superconducting symmetries using Josephson interferometry

W.K. Neils<sup>a,\*</sup>, D.J. Van Harlingen<sup>a</sup>, S. Oh<sup>a</sup>, J.N. Eckstein<sup>a</sup>, G. Hammerl<sup>b</sup>,  
J. Mannhart<sup>b</sup>, A. Schmehl<sup>b</sup>, C.W. Schneider<sup>b</sup>, R.R. Schulz<sup>b</sup>

<sup>a</sup> *Department of Physics, University of Illinois at Urbana-Champaign, 1110 West Green Street, Urbana, IL 61801, USA*

<sup>b</sup> *Center for Electronic Correlations and Magnetism, Institute of Physics, University of Augsburg, D-86135 Augsburg, Germany*

Unconventional superconductors are well known to have d-wave pairing symmetry characterized by a phase and magnitude anisotropy [1–3]. This anisotropy leads to instabilities of the d-wave order parameter at surfaces, vortex cores, magnetic impurities, and other interfaces, and could allow for the formation of a secondary pairing

symmetry not favored in the bulk material. If present, it is predicted that these surface regions will form a complex order parameter that breaks time-reversal symmetry. This offers unique systems to study novel superconducting states and will be important to the implementation of high- $T_c$  materials into electronic devices and systems.

The fragile nature of the d-wave order parameter near interfaces arises from the  $\pi$  phase difference between orthogonal crystal directions. A quasiparticle undergoing specular reflection at a

---

\* Corresponding author. Fax: +1-217-244-2278.  
E-mail address: neils@uiuc.edu (W.K. Neils).

(1 1 0) interface will see this  $\pi$  phase difference and, through Andreev reflection, form zero energy bound states (ZEBS) [4]. Evidence for the existence of these bound states in cuprate materials is observed as a peak in the conductance at zero energy in tunneling experiments and as modifications to the low temperature penetration depth [5–10]. It is the occupation of the ZEBS that suppresses the d-wave order parameter and allows for the emergence of a secondary pairing interaction that could form a complex order parameter at the interface [11]. Observation of spontaneous splitting of the zero energy conductance peak with decreasing temperature could be explained by broken time reversal symmetry consistent with a complex order parameter at the surface [12]. Similar effects are predicted in cuprate systems at interfaces with magnetic impurities. At low enough temperatures, islands of complex  $d_{x^2-y^2} + id_{xy}$ , formed around the magnetic impurities, could couple together causing a bulk transition to a complex phase. This mechanism is a possible explanation for an observed drop in the low temperature thermal conductivity in Ni-doped BSCCO, consistent with the order parameter becoming fully gapped [13,14].

The ideal method for identifying a pairing symmetry is to measure the relative phase between two crystal directions by measuring the magnetic diffraction pattern of a corner SQUID or a corner Josephson junction. The tunnel junctions are excellent directional probes and only sample the surface within a few coherence lengths. Relative phase drops between the two junctions shift the diffraction patterns allowing the phase to be measured accurately. The onset of a complex order parameter in the cuprate materials is expected to occur most strongly at the (1 1 0) face perpendicular to the order parameter node. Due to the difficulty in obtaining flat, undamaged (1 1 0) surfaces on single crystal samples, we cannot fabricate a corner SQUID or junction that samples the node direction. Instead we have chosen to use thin film grain boundaries to form an interface along this direction. These grain boundary junctions are formed by fabricating a cuprate film on a bi-crystal substrate, where one side of the substrate has been rotated by 45 degrees relative to the other such that the grain boundary forms along the (1 1 0)

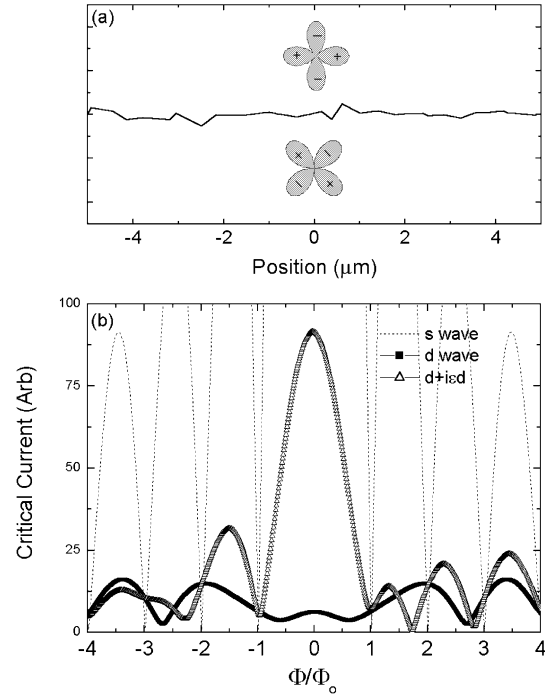


Fig. 1. (a) A simulation of a faceted 45-degree asymmetric grain boundary junction showing the relative orientation of the d-wave order parameter. (b) Diffraction patterns calculated from the grain boundary shown in part (a) showing the symmetric s-wave and d-wave cases and the asymmetric  $d + id$  wave case.

face. The resistively shunted Josephson junction forms naturally at the grain boundary and has a highly faceted interface caused by growth islands of competing orientation at the boundary [15]. Fig. 1(a) shows a diagram of a 45-degree asymmetric faceted grain boundary junction along with the orientation of the d-wave order parameter on either side of the junction. The faceted boundary acts like many corner junctions in parallel making the transport properties of the junction dependent on the order parameter anisotropy of the cuprate material. The  $\pi$  phase shift in the d-wave order parameter causes a highly structured, non-Fraunhofer diffraction pattern. Using a simple model in which the local critical current at each facet is determined by the product of the magnitude of the order parameters and the sine of the relative phase drop across the facet, we have simulated these junctions and calculated the diffraction pattern for

many different order parameters [16]. Fig. 1(b) shows the magnetic diffraction patterns, calculated for the faceted boundary shown in Fig. 1(a), for s-wave, d-wave, and  $d + i\epsilon d'$  symmetries. For the s-wave case, the isotropic order parameter removes any effects from the boundary facets and the usual Fraunhofer pattern is calculated. The nodes and the  $\pi$  phase shift in the d-wave case cause the facets to cancel reducing the overall magnitude of the critical current and produces a complicated modulation with applied field. It is important to note that the calculated diffraction pattern for the d-wave case, while reduced, is still symmetric in the short junction limit, but the maximum critical current does not occur at zero applied magnetic field. The modulation with applied magnetic field is a signature of the facet distribution and is different for each junction. When the order parameter becomes complex, the nodes are removed and the phase drop between orthogonal directions is between 0 and  $\pi$ . The diffraction pattern for the  $d + i\epsilon d'$  ( $\epsilon = 0.1$ ) case shows a dramatic increase in the zero field critical current along with significant asymmetries between the positive and negative field directions. The increase is expected because the order parameter becomes fully gapped when a secondary component is added in a complex way while the asymmetry with field polarity is a direct result of broken time-reversal symmetry of a complex order parameter.

We have previously measured YBCO grain boundary junctions and found no indication of a change in order parameter [16]. Fig. 2(a) shows measured magnetic diffraction patterns at several temperatures for a 20  $\mu\text{m}$  optimally doped  $\text{YBa}_2\text{Cu}_3\text{O}_{7-\delta}$  junction. Symmetric, non-Fraunhofer diffraction patterns were obtained for all temperatures measured, indicating d-wave pairing symmetry down to 1.5 K. We also measured several Ni-doped YBCO films in an effort to observe any bulk transition of the order parameter due to magnetic impurities. Fig. 2(b) shows magnetic diffraction patterns at several temperatures for a 10 micron  $\text{YBa}_2\text{Cu}_{2.85}\text{Ni}_{0.15}\text{O}_{7-\delta}$  junction. Again, we see symmetric, non-Fraunhofer diffraction patterns down to a temperature of 0.34 K, consistent with pure d-wave symmetry. Similar results are seen for other Ni concentrations.

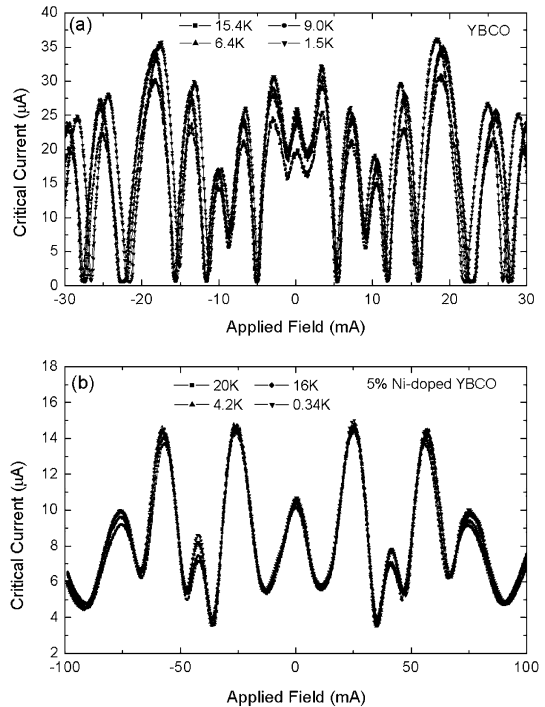


Fig. 2. Magnetic diffraction patterns for (a) a 20 micron YBCO junction and (b) a 10 micron 5% Ni-doped YBCO junction. Neither diffraction pattern shows any large asymmetry and is consistent with a pure d-wave order parameter.

It is possible that no complex order parameter is observed because the conditions at the interface are not conducive to the nucleation of a secondary superconducting phase. In an effort to change the properties near the grain boundary junctions, we have doped the YBCO films with a series of different impurities. Tunneling studies in Pr-doped YBCO wave show the zero-bias conductance peak is reduced as the Pr content is increased. Fig. 3(a) shows the magnetic diffraction patterns for a 10 micron  $\text{Y}_{0.8}\text{Pr}_{0.2}\text{Ba}_2\text{Cu}_3\text{O}_{7-\delta}$  junction on a 45-degree asymmetric STO substrate. At 40 K, the magnetic diffraction pattern is symmetric, consistent with d-wave symmetry. As the sample is cooled the magnetic diffraction pattern becomes distinctly asymmetric and the zero field critical current increases. To check that time-reversal symmetry is being broken, we reverse both the junction current and the magnetic field current and measure the junction again. This is equivalent to

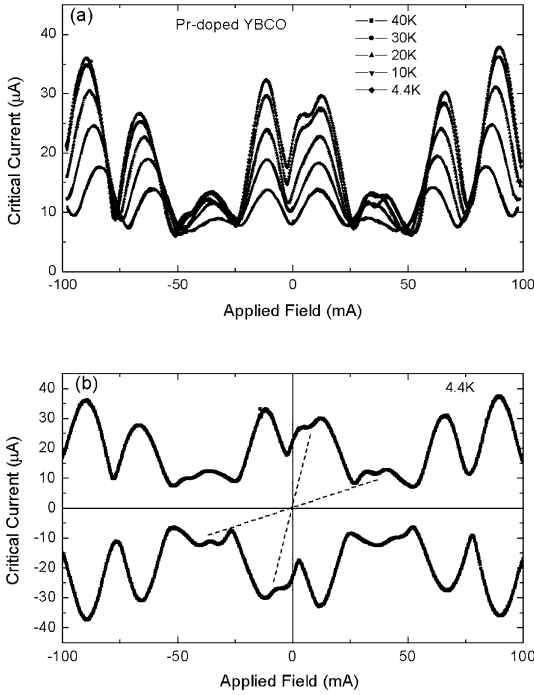


Fig. 3. Magnetic diffraction patterns for (a) a 10 micron 20% Pr-doped YBCO junction from 40 to 4.4 K and (b) both positive and negative critical current at 4.4 K. Asymmetries in the patterns are symmetric through the origin indicating no broken time-reversal symmetry. These asymmetries are caused by self-field effects.

reversing time. Fig. 3(b) shows both the positive and negative magnetic diffraction patterns for the same junction at 4.4 K. On this graph, time-reversal symmetry shows up as symmetry through the origin. All the asymmetric features in Fig. 3(b) show the same symmetry through the origin indicating the asymmetry is not caused by broken time-reversal symmetry expected from a complex order parameter. These asymmetries are due to self-field effects and they grow in strength with increasing critical current as the temperature decreases. It is not enough for there to be an asymmetry, it also must be time-reversed asymmetric.

Doping with certain materials can affect the carrier doping in the  $\text{CuO}_2$  planes and has a large effect on the barrier properties [17]. It has been shown that partial replacement of  $\text{Y}^{3+}$  in YBCO with  $\text{Ca}^{2+}$  causes the  $\text{CuO}_2$  planes to be overdoped

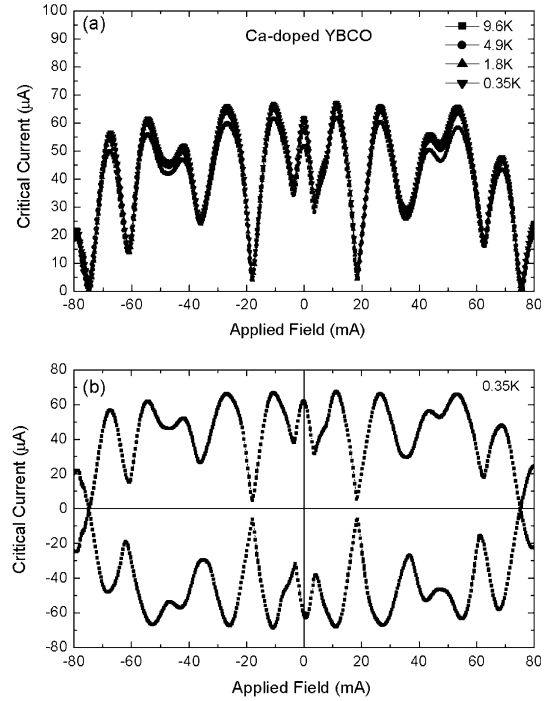


Fig. 4. Magnetic diffraction patterns for (a) a 15 micron 30% Ca-doped YBCO junction showing no large asymmetries and (b) both positive and negative critical current at 0.35 K. Small asymmetries are symmetric through the origin indicating they are not due to time-reversal symmetry breaking.

and increases the critical current density across grain boundaries. Conversely, partial replacement of  $\text{Cu}^{2+}$  with  $\text{Co}^{3+}$  underdopes the  $\text{CuO}_2$  planes and decreases the critical current density [18]. We have measured junctions with both Ca and Co doping in an effort to induce a secondary order parameter. Fig. 4(a) shows the magnetic diffraction pattern for a 15  $\mu\text{m}$   $\text{Y}_{0.7}\text{Ca}_{0.3}\text{Ba}_2\text{Cu}_3\text{O}_{7-\delta}$  junction on a 45-degree asymmetric STO substrate for several temperatures. The magnitude of the critical current is larger than the pure YBCO, consistent with Ca doping in other grain boundaries. There are no significant asymmetries seen in this junction. Fig. 4(b) shows both the negative and positive magnetic diffraction patterns for the same junction at 0.35 K. The small asymmetry near zero field is symmetric through the origin indicating pure d-wave with small self-field effects. Fig. 5(a) shows the magnetic diffraction pattern for

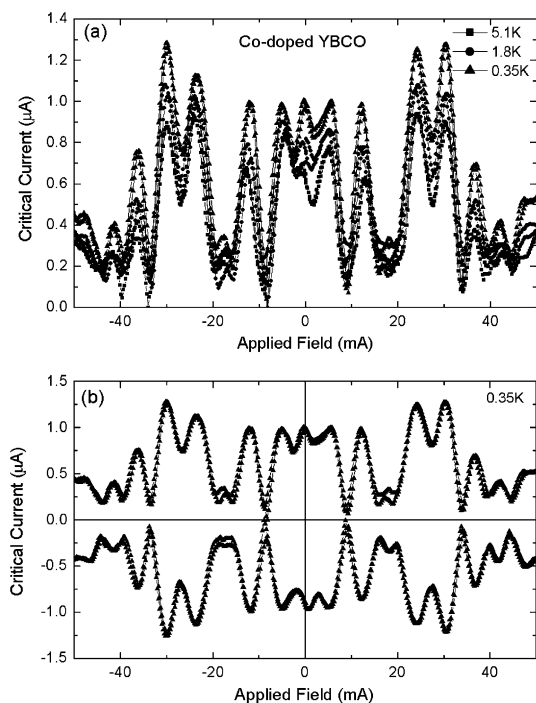


Fig. 5. (a) Magnetic diffraction patterns for a 20 micron 10% Co-doped YBCO junction. The junction was voltage biased to measure the current modulation and the data fit to a resistively shunted junction model to see the structure. (b) Magnetic diffraction patterns for both positive and negative critical current at 0.35 K.

a 20  $\mu\text{m}$   $\text{YBa}_2\text{Cu}_{2.9}\text{Co}_{0.1}\text{O}_{7-\delta}$  junction. The magnitude of the critical current in this junction was reduced, around  $1 \mu\text{A}$ , consistent with Co doping in other grain boundaries and was difficult to measure. The critical current was extracted from the current measured at a voltage criterion of  $10 \mu\text{V}$  using an RSJ model. There are some asymmetries in the pattern near zero field but they seem to become more symmetric with decreasing temperature. Fig. 5(b) shows the check of time reversal symmetry for the same junction at 0.35 K. There are some small asymmetries that are mirror symmetric (about the  $y = 0$  axis) consistent with broken time-reversal symmetry but they do not appear to grow stronger with decreasing temperature. These asymmetries are consistent with trapped vortices in the film near the junction that couple flux into the junction.

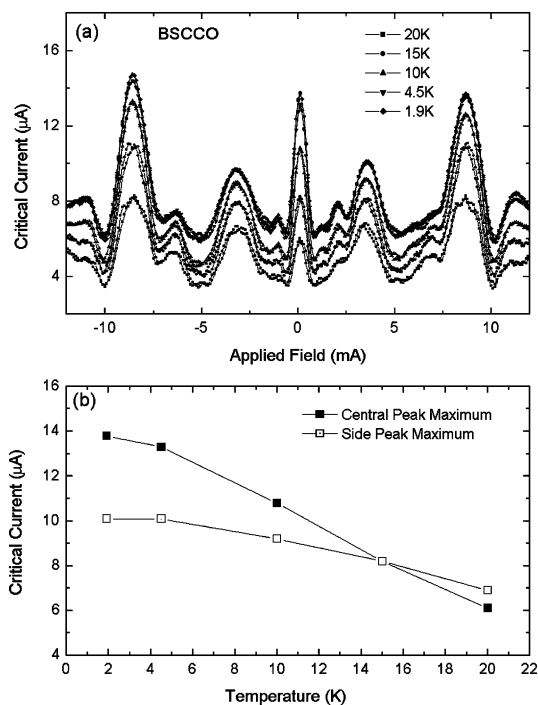


Fig. 6. (a) Magnetic diffraction patterns for a 30 micron BSCCO junction from 20 down to 1.9 K. As the temperature decreases, the critical current peak at zero field increases at a faster rate than other peaks in the pattern. (b) The critical current maximum of the central peak and the side peak, centered at 3.5 mA, plotted as a function of temperature.

Besides doping, the properties of the grain boundary will be affected by the growth process and the cuprate material being grown. In an effort to test this, we have measured transport properties of BSCCO grain boundary junctions grown by layer-by-layer molecular beam epitaxy (MBE) which yields atomically flat films. Fig. 6(a) shows the magnetic diffraction patterns for a 30  $\mu\text{m}$  BSCCO junction at temperatures from 20 down to 1.9 K. There are no large asymmetries appearing with decreasing temperature, consistent with pure d-wave symmetry over the temperature range measured. We do observe a peak in the critical current at zero field which increases more rapidly with decreasing temperature than any of the other peaks in the diffraction pattern as shown in Fig. 6(b). This is in contrast with other grain boundary junctions we have measured in which all of the

peaks in the diffraction pattern have the same temperature dependence and maintain their relative size. The most striking feature of this peak is that its width is precisely half the width of the other peaks in the diffraction pattern. Since we expect the minimum field feature size to be set by the magnetic junction area, we believe this is most likely due to a  $\sin(2\phi)$  component in the current–phase relationship. Current–phase relationships with periodicity  $2\phi$  have been predicted for tunneling in the node direction for which the first order tunneling into the plus and minus lobes cancels [19–21] and recent measurements of this relationship in YBCO grain boundary junctions have also shown similar  $2\phi$  components [22]. The MBE junctions may be more likely to show effects of higher order due to their cleaner and flatter grain boundary interfaces.

We have shown that transport properties of grain boundary Josephson junctions should be sensitive to changes in pairing symmetry predicted to occur in d-wave materials. Previously we have reported no evidence of complex order parameter at the grain boundary surface in YBCO or for a bulk transition to a complex order parameter in Ni-doped YBCO [16]. Attempts to change the character of the grain boundary interface in YBCO by doping with Pr, Ca, and Co have also shown no evidence of broken time-reversal symmetry. Diffraction patterns from a grain boundary Josephson junction grown by MBE show a peak at zero applied field with anomalous temperature dependence and short modulation length possibly consistent with a  $\sin(2\phi)$  component of the current–phase relationship.

## Acknowledgements

This work supported by NSF DMR99-72087, DEFG02-96ER45439, and BMBF-13N6918. The author would like to thank X. Yu and L.H. Greene for fabricating the Pr-doped YBCO samples.

## References

- [1] D.A. Wollman et al., Phys. Rev. Lett. 71 (13) (1993) 2134.
- [2] C.C. Tsuei et al., Phys. Rev. Lett. 73 (4) (1994) 593.
- [3] D.J. Van Harlingen, Rev. Mod. Phys. 67 (1995) 515.
- [4] C.-R. Hu, Phys. Rev. Lett. 72 (10) (1994) 1526.
- [5] M. Covington et al., Phys. Rev. Lett. 79 (2) (1997) 277.
- [6] A. Carrington, Phys. Rev. Lett. 86 (6) (2001) 1074.
- [7] J. Geerk et al., Z. Phys. 73 (1988) 329.
- [8] J. Leseuer et al., Physica C 191 (1992) 325.
- [9] H. Walter et al., Phys. Rev. Lett. 80 (16) (1998) 3598.
- [10] L. Alff et al., Euro. Phys. J. B 5 (1988) 423.
- [11] L.J. Buchholts et al., J. Low Temp. Phys. 101 (1995) 1079.
- [12] M. Fogelstrom, D. Rainer, J.A. Sauls, Phys. Rev. Lett. 79 (1997) 281.
- [13] A.V. Balatsky, Phys. Rev. Lett. 80 (9) (1998) 1972.
- [14] R. Movshovich et al., Phys. Rev. Lett. 80 (9) (1998) 1968.
- [15] H. Hilgenkamp, J. Mannhart, B. Mayer, Phys. Rev. B 53 (21) (1996) 14586.
- [16] W.K. Neils, D.J.V. Harlingen, cond-mat/0105388, submitted to Phys. Rev. Lett.
- [17] H. Hilgenkamp, J. Mannhart, Appl. Phys. Lett. 73 (2) (1998) 265.
- [18] G. Hammerl et al., IEEE Trans. Appl. Supercond. 11 (2001) 2830.
- [19] W. Zhang, Phys. Rev. B 52 (1995) 3772.
- [20] Y. Tanaka, S. Kashiwaya, Phys. Rev. B 53 (18) (1996) R11957.
- [21] Y. Tanaka, Phys. Rev. Lett. 72 (24) (1994) 3871.
- [22] E. Il'ichev et al., Phys. Rev. Lett. 86 (23) (2001) 5369.